2022

Evaluation of the Potential of Nanofluids Containing Different Ag Nanoparticle size Distributions for Enhanced Solar Energy Conversion in Hybrid Photovoltaic-Thermal (PVT) Applications

James Walshe
Technological University Dublin, james.walshe@tudublin.ie

John Doran
Technological University Dublin, john.doran@tudublin.ie

George Amarandei
Technological University Dublin, george.amarandei@tudublin.ie

Recommended Citation

Walshe. J., Doran, J. & Amarandei, G. (2022). Evaluation of the potential of nanofluids containing different Ag nanoparticle size distributions for enhanced solar energy conversion in hybrid photovoltaic-thermal (PVT) applications. *Nano Express*, vol. 3, no. 1. doi:10.1088/2632-959X/ac49f2

Funder: European Space Agency

Evaluation of the potential of nanofluids containing different Ag nanoparticle size distributions for enhanced solar energy conversion in hybrid photovoltaic-thermal (PVT) applications

To cite this article: J Walshe *et al* 2022 *Nano Ex.* **3** 015001

NANO EXPRESS

OPEN ACCESS

RECEIVED
9 November 2021

REVISED
6 January 2022

ACCEPTED FOR PUBLICATION
10 January 2022

PUBLISHED
19 January 2022

PAPER

Evaluation of the potential of nanofluids containing different Ag nanoparticle size distributions for enhanced solar energy conversion in hybrid photovoltaic-thermal (PVT) applications

J Walshe[1,2,3], J Doran[1,2,3] and G Amarandei[1,2]

[1] School of Physics & Clinical & Optometric Sciences, Technological University Dublin, City Campus, Grangegorman, Dublin, Ireland
[2] The Group of Applied Physics, School of Physics & Clinical & Optometric Sciences, Technological University Dublin, City Campus, Grangegorman, Dublin, Ireland
[3] Dublin Energy Lab, Environmental Sustainability and Health Institute, Technological University Dublin, City Campus, Grangegorman, Dublin, Ireland

E-mail: george.amarandei@tudublin.ie

Keywords: photovoltaics, solar thermal, PV/T system, Ag nanoparticles, nanofluid, modelling, heat transfer fluid

Abstract

Hybridising photovoltaic and photothermal technologies into a single system that can simultaneously deliver heat and power represents one of the leading strategies for generating clean energy at more affordable prices. In a hybrid photovoltaic-thermal (PVT) system, the capability to modulate the thermal and electrical power output is significantly influenced by the spectral properties of the heat transfer fluid utilised. In this study, we report on one of the first experimental evaluations of the capability of a multimodal silver nanofluid containing various particle shapes and particle sizes to selectively modulate the solar energy for PVT applications. The diverse set of particle properties led up to a 50.4% enhancement in the solar energy absorbed by the nanofluid over the 300 nm—550 nm spectral region, where silicon is known to exhibit poor photovoltaic conversion performances. This improved substantially the absorption of solar energy, with an additional 18–129 W m^{-2} of thermal power being generated by the PVT system. Along with the advancements made in the thermal power output of the PVT system, a decrease of 4.7–36.6 W m^{-2} in the electrical power generated by the photovoltaic element was noted. Thus, for every ∼11 W m^{-2} increase of thermal power achieved through the addition of the nanoparticles, a reduction of ∼3 W m^{-2} in the ability to generate clean electricity was sustained by the PVT. Despite the energy trade-offs involved under the conditions of the nanofluid, the PVT system cumulatively harvested 405 W m^{-2} of solar energy, which amounts to a total conversion efficiency of 45%. Furthermore, the economics of the additional energy harvested through merging of the two systems was found to reach an enhancement of 77% under certain European conditions.

1. Introduction

To progressively continue the process of decarbonizing the European economy, the European Union (EU) has established an ambitious set of energy targets for the sustainable production of electricity and thermal energy. For example, by 2030 the EU intends to sustain 20% of its electrical demand through photovoltaics (PV) and at least 49% of its residences demand for heating and cooling by renewable energy sources such as photothermal (PT) systems [1, 2]. However, by the end of 2020, 76% of the dwellings energy expenditure on heating and cooling was still met by the consumption of fossil fuels [2]. On top of this, in spite of an increased uptake in solar capacity, photovoltaics were only responsible for the production of 5% of the total power generated in the same year [3]. Consequently, the current rates of growth experienced in PV and PT uptake must become significantly increased over the coming years to reach the envisioned energy targets by 2030.

Cogeneration applications such as photovoltaic-thermal (PVT), which are capable of producing electrical power and heat simultaneously, represent one of the leading candidates for achieving the EU 2030 energy targets. In such a hybridized system, the 'waste heat', which is typically generated as a byproduct of the solar energy converted through the photovoltaic process, can be harvested to meet a larger proportion of the energy requirements of a residence [4, 5]. Furthermore, through the removal of any excess thermal energy from the PV system, an improved PV performance is expected as thermal energy is often considered detrimental to the energy harvesting efficiency of the PV collector [6, 7]. Thus, while the maximum conversion efficiency typically achieved with standalone PV and PT collection systems is 24.4 $\pm$ 0.5% and $\sim$50%, respectively [8, 9], a PVT unit could harvest from 30% to even 95% of the solar energy available [10, 11].

Within a classical PVT system, the removal of heat from the PV element is typically facilitated by the utilization of a heat transfer fluid (HTF) which acts as a thermal reservoir for the absorption and collection of thermal energy. This thermal reservoir is usually placed behind the PV as a cooling system with no direct interaction with the incoming solar radiation [12]. As a result, the properties of the 'working fluid' will influence the operability of the coupled system [13, 14]. Conventionally, heat transfer fluids have embodied liquids which were abundantly available and/or were cheap to produce in large quantities [15, 16]. Such liquids have included water, ethylene glycol, and mineral oils. These types of HTFs originally allowed PVT systems to progress in terms of the efficiencies achieved and reduced the costs involved in the unification process [17, 18]. An alternative solution is to place the HTF in front of the PVT [19], however, for this configuration to yield a positive exergetic merit for the system the spectral properties of these HTF needs to be carefully assessed before their integration in PVT applications [20]. This stems from the fact that in order to efficiently partition the solar spectrum into its respective thermal and electrical components, the optical properties of the HTF must also be spectrally matched to the responsivity of the PV element [21, 22]. Additionally, the ability of the classic HTFs to transport thermal energy efficiently can be restricted by their relatively low thermal conductivities [23]. These issues can be tackled by exploiting the capability of nanoparticles to modulate light-matter interactions at the nanoscale. Thus, the thermal and/or optical properties of a base fluid (any conventional liquid) can be selectively augmented to increase its performance [24, 25]. This can allow for conventional HTFs such as water to be repurposed for high-performance PVT applications through careful control and consideration of the nanoparticles size, shape, and distribution throughout the base fluid [26, 27]. The majority of the nanofluids investigated and reported in the literature so far have largely focused on exploiting a narrow and monomodal size distribution of nanoparticles including the shape and/or composition [28, 29]. This monomodal approach toward developing nanofluids has largely overlooked the possibility of combining a variety of different particle geometries, particle sizes, and/or compositions which could further enhance the eligibility of nanofluids for PVT applications [30, 31].

A nanofluid with a multimodal nanoparticle configuration has the ability to outperform a purely monomodal derivative of the same base fluid, when employed as a HTF in a PVT system. This ability stems from a number of key observations. Firstly, the wavelength response of the optical coupling mechanism that exists between the nanoparticles and the incoming solar flux (known as localised surface plasmon resonance or LSPR) is primarily restricted via the particle's size and/or morphology [32]. Thus, a wider distribution of the particle sizes becomes favourable for a nanofluid to effectively absorb a broader range of spectral frequencies for the purposes of energy harvesting. In addition, it has also been shown that the interparticle interactions (that can occur between neighbouring nanoparticles) in such a working fluid, under certain conditions, could significantly enhance thermal transport [33, 34]. Furthermore, the highly localised electromagnetic fields (EMF) that are established under LSPR are sensitive to deviations in the electromagnetic properties of the surrounding environment. This sensitivity can be advantageous. Thus, under a scenario where a wide distribution of different particle sizes and/or different particle shapes is employed, the strength of the highly localised EMFs established via LSPR at the nanoparticle's surface can be intensified by orders of magnitude [35]. The presence of such intensified EMFs in a HTF could lead to additional enhancements in the thermal performance of nanofluids, especially as more and more hybridizing options become available. The majority of these features can have a positive impact. However, they can also counteract each other and could combine to decrease the total energy harvested. This is why it is vitally important to understand the role played by each of these factors in influencing the modulation of the solar spectrum in a PVT system operating under static operating conditions. By removing the flow from the evaluation process, a clearer picture of how the fundamental optical and physical characteristics of the fluids are influencing the energy harvesting processes (i.e. 'thermal' and 'electrical') could potentially be elucidated. Although such hybridized nanofluids can often appear alluring from a fundamental scientific perspective, their economic impact on the overall exergetic performance of the collector often impedes their implementation into real-world energy harvesting applications. Consequently, as new nanofluids emerge as eligible candidates for hybrid PVT applications, all the criteria (i.e. including the economic ones) will be required to be evaluated when characterising the nanofluids behaviour in the energy harvesting system.

In this study, a water-based silver (Ag) nanofluid which contained a wide range of nanoparticle populations was explored as a possible heat transfer fluid for a monocrystalline silicon (mc-Si) based PVT system. The ability

of the Ag nanoparticles to modify the optical transmittance of the base fluid under differential loading conditions was examined experimentally using optical transmittance measurements. This allowed the spectral changes induced in the optical properties of the nanofluids to be ascertained. The impact of partitioning the solar spectrum into its thermal and electrical components for the PVT system, due to the presence of the nanofluids, was evaluated using modelling [21, 22]. Finally, the modified thermal and electrical power output of the PVT system under the partitioned solar irradiance of the nanofluids was analysed from an economic perspective through the implementation of a merit function [22]. In this regard, the economic merit of the additional energy captured as a result of modifying the spectral properties of the base fluid were analyzed under real-world European economic conditions.

2. Methods

2.1. Ag nanoparticle synthesis and the preparation of the nanofluid

A colloidal suspension containing silver (Ag) nanoparticles of various anisotropic particle shapes and particle sizes (diameter: 5–110 nm) was first synthesized using a two-step seed-mediated protocol that utilizes widely available and affordable chemical reagents [36]. This synthesis route was chosen as it has been previously explored for improving the thermal collection performance of solar thermal applications, the full details of this method being available in [37]. In the current study, for a typical synthesis procedure, 20 ml of silver nitrate (0.001 M) was employed during the 2nd stage of the synthesis process. This leads to a multimodal particle population in the nanofluid [37]. From the colloidal suspension produced, aliquots (of various volume) were taken and subsequently dispersed in a base fluid of ultrapure water ($\rho = 18.2\ \mathrm{M\Omega\ cm^{-1}}$) to produce loading concentrations of 0.05% to 10% volume-per-volume (v/v %) in 25 ml of the base fluid. This range of particle concentrations was selected based on the increased occurrence of stability issues in the nanofluid which were noted in the preliminary stability tests that were conducted at concentrations much larger than 10% volume-per-volume. These test results are in agreement with literature results [23, 24, 27, 33, 38] and show a decline in the PT/PVT performance and a decrease in the nanofluid stability as the concentration increases. The resulting series of Ag nanofluids were transferred to an ultrasonication bath for 30 min to reduce possible particle agglomeration prior to their optical characterisation and evaluation.

2.2. Optical and morphological characterisation of Ag nanofluids

The composition and optical behaviour of the water-based nanofluids in response to an increasing concentration of Ag nanoparticles were investigated using UV–vis spectroscopy, dynamic light scattering, and scanning electron microscopy. This collection of analysis techniques enabled not only the optical transmittance of the nanofluids to be determined, but also the underlying spectral components that result from the presence of different particle size-distributions and/or anisotropic particle morphologies to be resolved [37]. This aspect of the characterisation process is essential for the examination of the role played by the emergence and prevalence of different particle size-distribution populations on the resulting optical properties of the nanofluid.

The optical transmittance of the nanofluids was measured over the 300 nm—2000 nm spectral range using a Perkin Elmer Lambda 900 spectrometer (Perkin Elmer Inc. Massachusetts, USA) and employing 10 mm path length quartz cuvettes. Typically, to determine with a high degree of sensitivity the optical transmittance of a two-component fluid (such as the nanofluid investigated here) the transmittance measurement needs to be performed at two different path lengths [39]. However, the average deviation between the transmittance recorded at a single path length and the value registered using the standardised two path-length protocol outlined in [39] was found to be $\pm$ 6.4% for the analogous Ag nanofluid's described in [22]. Thus, the transmittance data presented herein correspond to spectra recorded using a single path-length, where the associated error on the measurement has been included in all subsequent calculations used in modelling that involve this spectral information.

The internal structure of the nanofluids (i.e. the diversity of the particle size-distributions present) was determined using both dynamic light scattering (DLS) and scanning electron microscopy (SEM). DLS measurements of the particle size were performed in triplicate using a Malvern Nano Series ZS Zetasizer (Malvern Instruments Ltd, Malvern, UK) which employed an illumination wavelength of 633 nm and a detector orientation of 173°. As a result, the error bar values included in the particle size figures represent the standard deviation across this series of triplicate measurements. In addition, the principles of derivative spectroscopy were applied to the DLS data to enhance the resolution of the spectral information attained using this technique. The complete details of this spectral processing procedure, including all the steps and criteria involved, can be found in [37]. To substantiate the particle information acquired using dynamic light scattering, SEM images of the particle morphologies existing within the nanofluids were captured using a Hitachi SU-6600 Field Emission

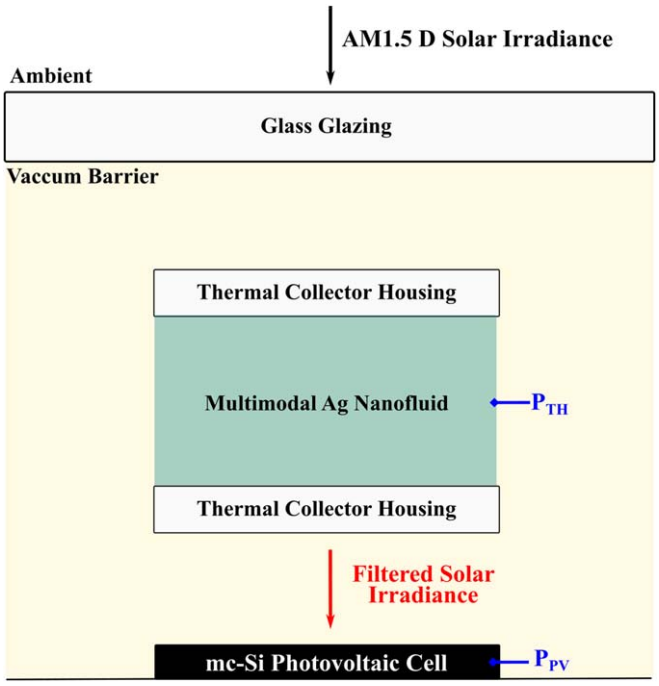

Figure 1. (a) Schematic of the photovoltaic-thermal (PVT) collector design formalised in the model indicating the different components in the design and the different outputs of the model i.e. the photovoltaic power (P_{PV}) and the thermal power (P_{TH}) produced under the optical conditions imposed by the multimodal Ag nanofluids considered in the study.

SEM (Hitachi Ltd, Tokyo, Japan). For the sample preparation technique and the image analysis the methodology described in [37] was used.

2.3. Merit function of PVT System with Ag nanofluids

The capability of the nanofluids to modulate and partition the solar spectrum into its respective 'thermal' and 'electrical' components within a photovoltaic-thermal (PVT) hybrid system was evaluated using the general accepted model described in [38]. This model was selected as it has been previously explored to evaluate the thermal and electrical conversion performances of a series of organic [21], organometallic [21], and composite nanofluids [22] when employed in an analogous PVT system design to that depicted in figure 1. The complete formalism of the model as well as an outline of where the empirical formula that underpin it were originally derived is provided in [21]. Hence, only a brief synopsis of the models input parameters, output metrics, and overall merit are included in the following discussion.

To evaluate the conversion efficiency of the thermal and electrical collection elements, the model requires a number of input parameters regarding the properties of the hybridised collection unit. Firstly, the spectral distribution of energy within the solar spectrum was integrated into the model through the inclusion of the standardised AM1.5D spectrum [40]. The optical interactions of the solar spectrum with the nanofluid (absorption, scattering and transmission) were incorporated into the model through the utilisation of the nanofluid's measured optical transmittance spectra [10, 21, 37, 39]. Finally, the capability of the transmitted solar flux to be converted into 'clean' electricity was calculated using the experimental spectral responsivity of the PV cell used in the PVT design i.e. in this case an aluminium-backed-surface-field monocrystalline silicon cell (Big Sun Community Solar, San Antonio, Texas, USA) [21, 22]

The amount of clean electrical power (P_{PV}) produced by the PVT system under the static filtered irradiance conditions of the various nanofluid configurations was determined via equation (1) [38]:

$$P_{PV} = FF \cdot V_{OC} \cdot \int \Phi_{AM1.5D}(\lambda) \cdot SR(\lambda) \cdot T_{Nanofluid}(\lambda) \cdot d\lambda \quad (1)$$

where SR is the spectral response of the mc-Si cell utilised, $\Phi_{AM1.5D}$is the spectral irradiance of the AM1.5D standard solar spectrum, $T_{Nanofluid}$ is the optical transmittance of the nanofluid (i.e. the transmittance spectra measured using the protocol outlined in section 2.2), and the fill factor (FF) and open-circuit-voltage (V_{OC}) of the mc-Si cell were determined through a series of equations which dictate its electrical behaviour [21, 22]. In addition, the lower and upper wavelength limits of the integral were taken as 300 nm and 2000 nm respectively, which corresponds to the limits of the recorded transmittance spectra.

Contrastingly, the amount of thermal power (P_{TH}) produced by the hybridised PVT collection system under static conditions was determined using equation (2) [38]:

$$P_{TH} = \eta_{Collector} \cdot \int \Phi_{AM1.5D}(\lambda) \cdot [1 - T_{Nanofluid}(\lambda)] \cdot d\lambda \quad (2)$$

Where [*1—*$T_{Nanofluid}$] equals the fraction of solar energy absorbed by the nanofluid due to its unique internal structure, $\Phi_{AM1.5D}$is the spectral irradiance of the AM1.5D standard solar spectrum, $\eta_{Collector}$ is the thermodynamic limit of efficiency for the energy harvesting process in a specific form of standardised collector geometry [38, 41], and the limits of the integration remain the same as that outlined for P_{PV}. Further adjustments to the thermal power that could potentially arise from the optimisation of the collector geometry and/or flow conditions imposed on the nanofluid in a non-static collection scenario (which would influence the $\eta_{Collector}$ term in equation (2) were not considered in this study. However, further studies will be needed to evaluate the effects of the concentration on the pressure drop and pumping power, but these studies are not falling within the objective of this work. For a nanofluid to truly offer a better alternative to conventional heat transfer fluids it must outperform the thermal and/or electrical behaviour of the base fluid (which is single-component fluid), when implemented in the PVT design. Thus, to make the comparison between the performances achieved with the base fluid (i.e. water in this investigation) and the nanofluid (under the different nanoparticle loading concentrations) easier to interpret, the variation between them was reported as:

$$Enhancement\ in\ P_{Electrical}(\%) = 100 \cdot [(P_{PV} - P_{PV_*})/(P_{PV_*})]$$

and

$$Enhancement\ in\ P_{Thermal}(\%) = 100 \cdot [(P_{PV} - P_{TH*}) / (P_{TH*})]$$

where P_{PV} and P_{TH} represent the electrical and thermal power produced under the conditions of the nanofluid, respectively, and P_{PV_*} and P_{TH*} correspond to the electrical and thermal power generated under the conditions of the base fluid, respectively. Although these improvements in the exergetic performance provide information on the correlation between the spectral modifications initiated in the nanofluids optical properties and the additional energy that is captured as a result, they do not consider the economic trade-offs involved in capturing this additional energy [17]. Hence, a merit function (*MF*) described by equation (3) which considers the price of electricity and thermal energy (available within a specific geographical region) was utilised to demonstrate the clear economic advantages of modifying the optical properties of the base fluid and/or retrofitting the standalone PV systems [21, 38]:

$$MF = (w \cdot P_{PV} + P_{TH}) / (w \cdot P_{PV\ (standalone)}) \quad (3)$$

Here, P_{PV} and P_{TH} represent the electrical and thermal power sustained, respectively; $P_{PV\ (standalone)}$ defines the electrical power produced by the PV element in the absence of any working fluid i.e. no base fluid or nanofluid is retrofitted to the collector design. Meanwhile, the worth factor (w) describes the ratio of the cost of electricity to the cost of thermal energy (10, 38). Therefore, the worth factor is highly sensitive to the localised energy marketplace found at a particular geographical location [21, 22]. For example, in Sweden the combination of an electricity price of € 0.1990 per kilowatt-hour (kW·h) and a thermal energy price of 0.1223 € $(kW{\cdot}h)^{-1}$ yield a worth factor value of 1.63 [42, 43]. In contrast, the average price of electricity and thermal energy in the domestic market of Germany is 0.3000 € $(kW{\cdot}h)^{-1}$ and 0.0608 € $(kW{\cdot}h)^{-1}$, respectively [42, 43]. This implies that the enhancements reported in P_{PV} and P_{TH} can be evaluated under real-world economic scenarios. From such scenario, the specific geographical locations for further evaluation of the PVT design can be strategically identified. In this investigation, the real-world economic scenarios under which the nanofluids were evaluated consisted of an average European climate ($w = 3.09 \pm 0.89$) and the conditions found in the Republic of Ireland ($w = 3.34$) [42, 43].

3. Results and discussion

3.1. Spectral characteristics of Ag nanofluids

As Ag nanoparticles were increasingly introduced into the base fluid by increasing the amount of aliquot to be inserted in the base fluid, very little change in the optical transparency of the resulting nanofluid was registered —see figure 2(a). Only at a loading concentration of 10% v/v a noticeable change in the visual appearance of the nanofluid was observed. This change in the optical behaviour of the nanofluid is expected to arise from the increased number of nanoparticles present within the fluid, which increases the favourability of aggregative and/or scattering processes [44, 45]. Indeed, the existence of larger-sized particles within the nanofluid was independently confirmed using SEM analysis. The wide range of particle sizes (5 nm–110 nm) observable in the SEM image of the particles shown in figure 2(b) demonstrates this attribute of the nanofluids internal structure. Additionally, in a former study of the synthesis route applied here, the ability of the protocol to yield a number of

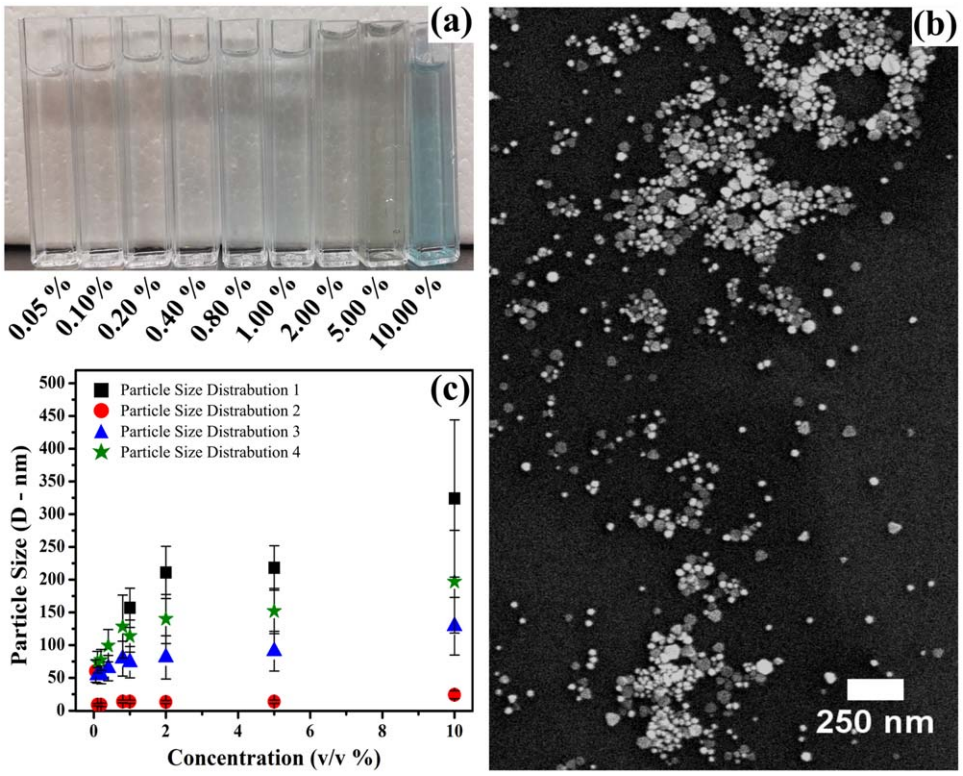

Figure 2. (a) Photograph of the silver nanofluid under the differential loading conditions showing the changes in its optical appearance. To be noted that the v/v% concentration refers to the percentage of aliquots (containing the nanoparticles) taken and subsequently dispersed in the base fluid (here, water) and not the nanoparticle concentration in the base fluid. (b) Typical SEM image (scale bar 250 nm) emphasizing the range of particle-sizes (5–110 nm) existing within the nanofluid at low (here, 0.05 v/v%) loading concentrations and (c) the emergence and expansion of the individual particle size distributions (PSD 1–4) present within the overall particle ensemble illustrated in panel (b) as the concentration of nanoparticles is increased.

distinct anisotropic particle morphologies including prisms, cubes, hexagons and other non-spherical geometries has been demonstrated [37].

The individual particle size-distributions that comprise the internal structure of the nanofluid under an increasing loading concentration are displayed in figure 2(c). For an Ag nanoparticle concentration below 0.5% v/v, the internal structure of the nanofluid primarily consisted of 3 distinct particle populations (figure 2(c)—PSD 2, PSD 3, and PSD 4) which contained particle sizes ranging from 5 nm to 125 nm. As the loading concentration is increased to 0.8% v/v, the maximum particle size within the particle network was extended to ∼175 nm (figure 2(c)—PSD 4—green star). The emergence of this concentration-dependent particle size behaviour could suggest that as more nanoparticles are incorporated into the nanofluid, the tendency of the nanofluid's internal structure to reconfigure to accommodate the competing interaction mechanisms available within the nanofluid is becoming more apparent. Hence, at loading concentrations exceeding 0.5 v/v%, the particle size distribution embodied by the nanofluids becomes increasingly divergent from the original particle size distribution that was contained in the aliquots of colloidal suspension created during the nanofluid's development. Indeed, this trend appears to be reflected in the data presented in figure 1(c) via the emergence of a new particle size population at 1% v/v (figure 2(c)—PSD 1, black square) for the nanofluids investigated. All these distinct distributions of particle sizes (PSD 1—PSD 4) are cumulatively responsible for the light-matter interactions within the nanofluid, and, thus, the corresponding optical transmittance spectra that is produced will be influenced by their presence. As more nanoparticles were dispersed throughout the nanofluid (i.e. 2% to 10% v/v), a competition between the different particle-size distributions existing within the nanofluid seems to occur mainly due to the dynamic evolution of aggregation processes that led to nanoparticle cluster formation [46].

As a result, a much more complex and expansive range of particle sizes (5 nm—440 nm) is produced within the particle network as illustrated in figure 2(c). It is this advantageous combination of a wide distribution of particle sizes that has been shown to enhance the magnitude of the light-matter interactions of metal nanoparticle-based nanofluids [47] and enhance their thermal conversion performances [22, 37]. Moreover, the various shapes of the particles demonstrated in figure 2(b) can also contribute to the enhancement in the solar energy conversion, but a systematic study on the role of the shape will be required to be performed in the future.

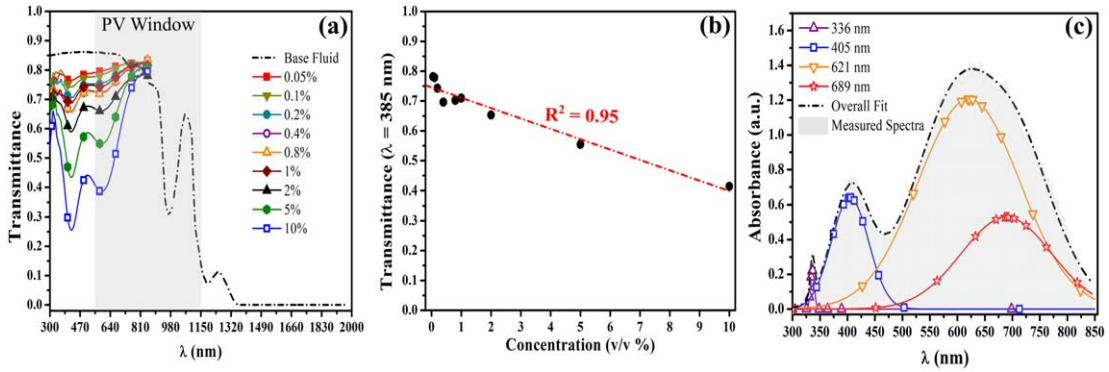

Figure 3. (a) Optical transmittance spectra of the various nanofluids and (b) the accompanying variation in the transmittance at $\lambda = 385$ nm as the loading concentration of nanoparticles is increased. The spectral bandwidth over which the mc-Si PV cell operates at close to peak conversion efficiencies ('PV Window') is also highlighted in panel (a) for comparison. (c) The individual spectral components responsible for the recorded transmittance spectrum in panel (a).

To effectively partition the solar spectrum and to ensure that the energy independently harvested by each type of collector in the PVT design is maximised, particular spectral bandwidths could be 'targeted' for absorption and the production of thermal energy. For the mc-Si cell utilised here these targeted bands of wavelengths corresponded to 300–550 nm (thermal window #1) and 1150–2000 nm (thermal window #2) [21, 22]. These unique bandwidths are defined based on their position lying outside of the region of the solar spectrum where the mc-Si PV cell is most efficient at harvesting electrical energy i.e. 550 nm to 1150 nm (figure 3(a)—PV Window, grey fill area). As 0.05%—0.4% v/v of nanoparticles were introduced into the base fluid, a 9% (figure 3(a)—red square) to 18% (figure 3(a)—purple unfilled circle) increase in the solar energy absorbed by the nanofluid across thermal window #1 was observed due to increased absorption contributions of the nanoparticles. At this same concentration range only a small fraction (7.1–19.2 W m^{-2}) of the solar energy falling within the PV window was sacrificed due to the enhanced absorption response of the nanofluid. This optical response occurs because at these loading concentrations the relatively small number of individual particles distributions evident in figure 2(c) restrict the light-matter interactions primarily to the 300–550 nm part of the solar spectrum (see figure 3(a)). However, it is expected that as both the number and the size of the individual particle size distributions grow in accordance with the increasing concentration of nanoparticles dispersed throughout the nanofluid (figure 2(c)), the extent of this optical interaction extends further into the red part of the spectrum.

Expanding the concentration above 0.4% v/v yielded up to an additional 108 W m^{-2} of solar energy being absorbed from thermal window #1, which represents a 50.4% improvement (figure 3(a)—10% v/v, blue unfilled square) over the performance of the base fluid in the same spectral region. In terms of the energy trade-off involved in sustaining this improved absorption capability of the nanofluid, up to ~73 W m^{-2} of the solar energy originally transmitted through the base fluid within the PV window is repurposed for the generation of thermal energy at this concentration. This represents an ~18% reduction in the solar irradiance reaching the PV cell in the PVT design. Thus, it is expected that the outputs of the model (i.e. $P_{PV}$and P_{TH}) will reflect the trend of thermal and electrical behaviour.

The correlation between the transmittance (measured at a wavelength of 385 nm which is within thermal window #1) and the loading concentration of the nanoparticles employed in the nanofluid was found to obey a linear relationship as illustrated in figure 3(b). With the exception of some minimal perturbations occurring over concentrations less than 1% v/v, the linear response of the nanofluid to an increasing loading concentration is maintained ($R^2 = 0.95$). This implies that the nanoparticles remain uniformly dispersed throughout the base fluid, and there are no indications of large-scale aggregates forming or sedimentation processes commencing within the nanofluid. However, once deconvoluted, the absorption spectra of the different nanofluids revealed the presence of a number of distinct spectral components which were contributing to the spectral information presented in figure 3(a). An example of a deconvoluted absorption spectrum is provided in figure 3(c). Considering the relationship between the size of a nanoparticle and its resulting LSPR absorption peak [46], it is possible that the different spectral components registered in the deconvoluted spectrum shown in figure 3(c) could correspond to the number of particle size-distributions outlined in figure 2(c). This relationship would suggest that the interplay between the different particle size-distributions of the nanofluid could potentially be correlated to specific spectral markers that occur within the absorption spectrum of the nanofluid. However, such an investigation is outside the scope of this work.

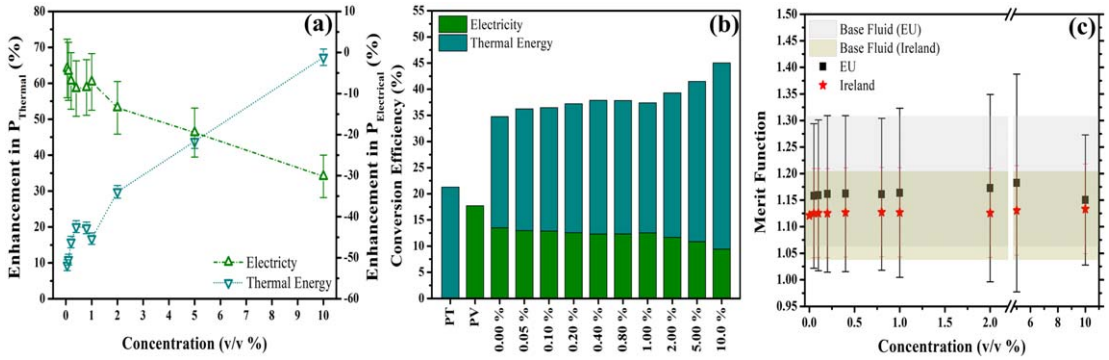

Figure 4. (a) The enhancement of the electrical power (upright triangle) and thermal energy (inverted triangle) produced by the PVT system under the different loading conditions of the nanofluid. (b) The absolute combined conversion efficiency of the solar energy using both technologies (thermal & electrical), where the performances of these standalone collection devices (i.e. PV and PT) are included for comparison. (c) The merit function value of the nanofluids under EU (black square) and Irish (red star) economic conditions. The performances of the base fluid (i.e. 0 v/v %) in each scenario are also included as a grey-fil-area and a yellow-fill-area, respectively.

3.2. Solar energy conversion performance of PVT system with Ag Nanofluids

The translation of the optical behaviour reported in figure 3(a) into the corresponding variations in the electrical and thermal power produced by the PVT system is demonstrated in figure 4(a). In correspondence with the linear relationship identified between the nanofluid's loading concentration and the variation in its absorption profile (figure 3(b)), an almost linear ($R^2 = 0.94$) enhancement in the thermal power output in response to an increasing nanoparticle concentration can be seen in figure 4(a) (inverted triangles). Thus, as more nanoparticles are added to the nanofluid, the amount of solar radiation that is absorbed and converted by the nanofluid into thermal energy is increasing (figure 4(a) and 4 (b)). The rate of this enhancement in the thermal power produced by the nanofluid was found to be $5.7 \pm 0.5\%$ per unit increase in the volume-per-volume loading concentration (figure 4(a)). Hence, by integrating a diverse series of nanoparticle sizes a 7.9% (0.05% v/v) to 69.5% (10% v/v) enhancement in the thermal power produced by the PVT system was achieved when compared to the base fluid.

Alongside these improvements in the thermal power output of the PVT system, a moderate decrease in the conversion efficiency of the PV element is also noted in figure 4(a) (upright triangles). This type of behaviour was expected as energy losses tend to typically be sustained by the PV component as more and more thermal energy is generated within the thermal collection element of the PVT system [38, 48]. Accordingly, the rate of decrease in the electrical power output of the PVT system (figure 4(a)—upright triangles) under the conditions of the nanofluid followed an almost perfectly linear relationship ($R^2 = 0.97$). Under this relationship, the conversion performance of the PV element decreased at a rate of $2.5 \pm 0.2\%$ per unit increase in the volume-per-volume loading concentration when compared to the base fluid. This resulted in up to a 35% reduction in the electrical power that was generated by the PVT system. A noticeable exception to this behaviour was reported at lower concentrations (0.05% to 0.10% v/v), whereby the increased scattering contributions of the nanofluids yielded a positive enhancement ($2\% - 3\%$) in the PV performance. In summary, an additional 18–129 W m^{-2} of thermal power can be generated by the PVT under the conditions of the nanofluid, at the expense of a 4.7–36.6 W m^{-2} reduction in the electrical power that is produced by the mc-Si cell.

Irrespective of the nanofluid, merging of the PT and PV systems increased the total energy harvested by the collection process from ~18% to ~35% (figure 4(b)—base fluid). This represents a 94% relative enhancement over the conversion performance achievable with the standalone mc-Si technology, which is also restricted by its ability to solely generate electrical energy. Through the addition of Ag nanoparticles, the total energy harvested by the PVT system is extended by an additional 1.5% (figure 4(b)—0.05% v/v) to 10.2% (figure 4(b)—10% v/v). Therefore, by controlling the loading concentration of the nanoparticles, and hence the internal structure of the nanofluid, up to 45% of the solar irradiance can potentially be absorbed and converted into electrical and thermal energy (figure 4(b)). It is feasible to consider that, through further refinement of the particle geometries, flow rate conditions, and the collector architecture, higher collector performances could potentially be achieved [13, 14, 25, 31, 49]. However, such investigations are outside the scope of this current work.

3.3. Merit function of Ag nanofluids

Under the EU economic conditions, combining the PV and PT systems provided not only an increased exegetic performance but also an improvement in the economic merit of the additional energy that was captured as a result. For example, the economic enhancement ranged from 6.3% in countries like Luxembourg, Croatia, and the UK up to 30.8% in France. Therefore, the Ag nanofluids must outperform these metrics to be considered as a

high-performance alternative to the single-phase heat transfer fluids in which the nanoparticles are dispersed, in this case, water. Under the constraints of the energy landscape of Bulgaria, Greece, France, and Italy the addition of the Ag nanoparticles into the base fluid yielded a 2.2% (0.05% v/v) to 13.8% (10% v/v) absolute enhancement in the economic merit of the additional energy captured. As the analysis was progressively moved towards countries with a higher worth factor such as Hungary ($w = 3.22$), Poland ($w = 3.10$), Slovakia ($w = 3.19$), and Ireland ($w = 3.34$, figure 4(c)—red stars) this enhancement reduced to 0.4% to 3.2%, respectively. Evaluating the exergetic merit of the nanofluids under the scenarios where the economic incentive to produce electricity was even higher (e.g. the UK), resulted in the addition of the nanoparticles having a negative economic impact on the performance. Thus, although the nanofluids contributed up to a 67% increase in $P_{Thermal}$, the relatively small reduction witnessed in the $P_{Electrical}$ of the PVT sustained under these economic conditions presents a limitation.

However, this does not disincentivise the unification of PV and PT technologies but rather restricts their application to economic climates that can potentially fully capitalise on the advantages of the additional energy that is produced. For example, in Sweden ($w = 1.63$) the comparably low price to deliver thermal energy relative to electricity increases the benefit of modifying the spectral properties of the base fluid. Under the economic conditions of the Swedish climate, the economic merit of the additional energy captured by the nanofluid becomes increased up to 27% (10% v/v) relative to the base fluid. To take this example to the extreme, let us consider a situation outside EU e.g. in China, where the worth factor has a value of ∼0.8 [50, 51]. In this case, the economic incentive to modify the spectral properties of the base fluid to capture an additional 10.2% of the solar irradiance (figure 4(b)) becomes intensified to 80%. Thus, under the spectral conditions of the nanofluid, the PVT collector could potentially harvest 45% of the solar energy and increase the worth of the additional energy captured by 80% if the collection unit were to be installed in the Chinese region. The comparison between the different performance enhancements elucidated when evaluating the nanofluids under different economic environments highlights the capability of the PVT model to identify specific geographic locations for the future implementation of nanofluid based PVT collection systems.

4. Conclusion

The capability of Ag nanofluids comprised of different particle sizes to increase the thermal power, cost effectiveness, and the combined conversion efficiency of an mc-Si based PVT system was systematically explored. The integration of this diverse set of particle properties into a base fluid of water resulted in an additional 21 W m^{-2} to 108 W m^{-2} of solar energy being absorbed by the nanofluid over the 300–550 nm spectral range. This high-energy region of the solar spectrum is typically inefficiently harvested by most commercial PV technologies, including mc-Si and, therefore, it is more suitable to be directed towards the production of thermal energy in the PVT system. Furthermore, a strong linear correlation was exhibited between the concentration of nanoparticles employed in the nanofluid's design and the additional solar power absorbed by the thermal collection unit. Under this relationship, the solar energy captured by the nanofluid was found to increase at a rate of ∼11 W m^{-2} per percentage increase in the v/v loading concentration. Thus, at the maximum loading concentration of 10% v/v, the nanofluid was capable of delivering a 50.4% improvement over the performance of the base fluid in the same spectral region. This improved capability to modulate and partition the solar spectrum resulted in an additional 18–129 W m^{-2} of thermal power being generated by the PVT system when the nanofluid is acting as the heat transfer fluid. However, for the nanofluids to retain their intensified absorption contribution within the spectral window targeted for the production of thermal energy, a moderate decrease in the performance of the PV element occurred. This decrease in PV performance corresponded to a loss of 4.7–36.6 W m^{-2} in electrical power for the PVT system, which represented a 4% to 30% decrease in the performance of the unmodified base fluid, respectively. Thus, for every percentage increase in the v/v loading concentration the conversion efficiency of the thermal collector can be increased at the expense of a 3.2 W m^{-2} reduction in the electrical power delivered by the PVT. Despite these limitations, the cumulative conversion efficiency of both systems working in tandem still exceeded that of the standalone photovoltaic and photothermal units by up to 31.5%. Thus, by synergistically combining a diverse nanoparticle population with a hybridisation strategy that combines PV and PT collection systems $\sim$ 405 W m^{-2} of solar energy could become harvestable for the production of electricity and thermal energy. The economic incentive to merge the independent collection systems into a single architecture and modify the spectral properties of the base fluid through the inclusion of the nanoparticles was also demonstrated under different European economic climates for the first time. The results of this novel economic analysis revealed how, by considering the energy landscape criteria, a 1% to 77% increase in the economic merit of the additional energy could potentially be achieved. In particular, economies whose worth factor exceeded ∼4.7 (e.g Belgium and Germany) were found to have a negative impact on the collection performance. This economic analysis thereby permits the expected

performance of the nanofluid equipped PVT system under the specific economic conditions found in niche European climates to be 'screened' in the prospect of identifying the most suitable environments for PVT implementation. In terms of the improvements in performance achieved with the nanofluids as compared to the base fluid, the economics of the additional energy harvested translated into a 0.1% to 26.7% economic enhancement. Accordingly, a higher degree of economic merit was recognized for economies where the worth factor fell below a value of 3. This included countries such as Bulgaria, Greece, France, the Netherlands, and Sweeden to name but a few within the EU region. The combination of enhanced absorption capabilities, improved thermal power output, increased energy harvesting, and more cost-effective economics suggests that these multimodal Ag nanofluids could potentially increase the performance of PVT systems.

Acknowledgments

The authors acknowledge the support from the European Space Agency who financed part of this project.

Data availability statement

The data that support the findings of this study are available upon reasonable request from the authors.

ORCID iDs

G Amarandei https://orcid.org/0000-0002-6648-6635

References

[1] Chevillard N *et al* 2020 EU market outlook for solar power 2020 – 2024 *Solar Power Europe* 10–20 https://www.solarpowereurope.org/european-market-outlook-for-solar-power-2020-2024/
[2] Questions and Answers-Making our energy system fit for our climate targets 2021 (European Commission) [Press Release]
[3] Energiewende A and Climate E 2021 The European power sector in 2020: up-to-date analysis on the electricity transition *Agora Energiewende and Ember Climate* 7–8 https://www.agora-energiewende.de/en/publications/the-european-power-sector-in-2020/
[4] Khordehgah N, Żabnieńska-Góra A and Jouhara H 2020 Energy performance analysis of a pv/t system coupled with domestic hot water system *Chem. Engineering.* **4** 22
[5] Özakın A N, Karsli S, Kaya F and Güllüce H 2016 The heat recovery with heat transfer methods from solar photovoltaic systems. *Journal of Physics: Conf. Series.;707* (https://doi.org/10.1088/1742-6596/707/1/012050)
[6] Amin A A E and Al-Maghrabi M A 2018 The analysis of temperature effect for mc-si photovoltaic cells performance *Silicon.* **10** 1551–5
[7] Dubey S, Sarvaiya J N and Seshadri B 2013 Temperature dependent photovoltaic (PV) efficiency and its effect on PV production in the world—a review *Energy Procedia* **33** 311–21
[8] Al-Shamani A N *et al* 2014 Nanofluids for improved efficiency in cooling solar collectors—A review *Renew. Sustain. Energy Rev.* **38** 348–67
[9] Green M, Dunlop E, Hohl-Ebinger J, Yoshita M, Kopidakis N and Hao X 2021 Solar cell efficiency tables (version 57) *Prog. Photovoltaics Res. Appl.* **29** 3–15
[10] Han X, Xue D, Zheng J, Alelyani S M and Chen X 2019 Spectral characterization of spectrally selective liquid absorption filters and exploring their effects on concentrator solar cells *Renewable Energy* **31** 938–45
[11] Othman M, Hussain F, Sopian K, Yatim B and Ruslan M H 2013 Performance study of air-based photovoltaic-thermal (PV/T) collector with different designs of heat exchanger *Sains Malaysiana.* **42** 1319–25
[12] Ahmed A, Baig H, Sundaram S and Mallick T K 2019 Use of nanofluids in solar PV/Thermal systems *Int. J. Photoenergy* **2019** 1–17
[13] Huang G, Curt S R, Wang K and Markides C N 2020 Challenges and opportunities for nanomaterials in spectral splitting for high-performance hybrid solar photovoltaic-thermal applications: A review *Nano Materials Science.* **2** 183–203
[14] Yazdanifard F, Ameri M and Taylor R 2021 Parametric investigation of a nanofluid-NEPCM based spectral splitting photovoltaic/thermal system *Energy Convers. Manage.* **240** 114232
[15] Choi S U and Eastman J A 1995 *Enhancing thermal conductivity of fluids with nanoparticles* Argonne National Lab, United States of America
[16] Srivastva U, Malhotra R and Kaushik S 2015 Recent developments in heat transfer fluids used for solar thermal energy applications *J Fundam Renew Energy Appl.* **5** 189
[17] Hassani S, Saidur R, Mekhilef S and Taylor R A 2016 Environmental and exergy benefit of nanofluid-based hybrid PV/T systems *Energy Convers. Manage.* **123** 431–44
[18] Kalidasan B, Divyabharathi R, Pandey A K and Saidur R 2021 Review on economic analysis of photovoltaic thermal systems *IOP Conf. Ser.: Mater. Sci. Eng.* **1127** 012008
[19] Liang H, Wang F, Yang L, Cheng Z, Shuai Y and Tan H 2021 Progress in full spectrum solar energy utilization by spectral beam splitting hybrid PV/T system *Renew. Sustain. Energy Rev.* **141** 110785
[20] Huang G, Wang K and Markides C N 2021 Efficiency limits of concentrating spectral-splitting hybrid photovoltaic-thermal (PV-T) solar collectors and systems *Light: Science & Applications.* **10** 28
[21] Walshe J, Carron P M, McCormack S, Doran J and Amarandei G 2021 Organic luminescent down-shifting liquid beam splitters for hybrid photovoltaic-thermal (PVT) applications *Sol. Energy Mater. Sol. Cells* **219** 110818
[22] Walshe J, Carron P M, McLoughlin C, McCormack S, Doran J and Amarandei G 2020 Nanofluid development using silver nanoparticles and organic-luminescent molecules for solar-thermal and hybrid photovoltaic-thermal applications *Nanomaterials (Basel)* **10** 1201

[23] Ali N, Teixeira J A and Addali A 2018 A Review on nanofluids: fabrication, stability, and thermophysical properties *Journal of Nanomaterials.* **2018** 6978130
[24] Wole-osho I, Okonkwo E C, Abbasoglu S and Kavaz D 2020 Nanofluids in solar thermal collectors: review and limitations *Int. J. Thermophys.* **41** 157
[25] Zain M *et al* 2021 Performance investigation of a solar thermal collector based on nanostructured energy materials *Frontiers in Materials.* **7** 462
[26] Maheshwary P B, Handa C C, Nemade K R and Chaudhary S 2020 Role of nanoparticle shape in enhancing the thermal conductivity of nanofluids *Mater. Today Proc.* **28** 873–8
[27] Rudyak V Y and Minakov A V 2018 Thermophysical properties of nanofluids *The European Physical Journal E.* **41** 15
[28] Elsaid K *et al* 2021 Thermophysical properties of graphene-based nanofluids *Int. Journal of Thermofluids.* **10** 100073
[29] Zeroual S *et al* 2020 Ethylene glycol based silver nanoparticles synthesized by polyol process: Characterization and thermophysical profile *Journal of Molecular Liquids.* **310** 113229
[30] Jamil F and Ali H M 2020 Chapter 6 - Applications of hybrid nanofluids in different fields *Hybrid Nanofluids for Convection Heat Transfer* ed H M Ali (New York: Academic) 215–54
[31] Wole-Osho I, Adun H, Adedeji M, Okonkwo E C, Kavaz D and Dagbasi M 2020 Effect of hybrid nanofluids mixture ratio on the performance of a photovoltaic thermal collector *Int. J. Energy Res.* **44** 9064–81
[32] Motl N E, Smith A F, DeSantis C J and Skrabalak S E 2014 Engineering plasmonic metal colloids through composition and structural design *Chem. Soc. Rev.* **43** 3823–34
[33] Karagiannakis N P, Skouras E D and Burganos V N 2020 Modelling thermal conduction in nanoparticle aggregates in the presence of surfactants *Nanomaterials (Basel).* **10** 11
[34] Kondaraju S, Jin E K and Lee J S 2011 Effect of the multi-sized nanoparticle distribution on the thermal conductivity of nanofluids *Microfluid. Nanofluid.* **10** 133–44
[35] Sun G and Khurgin J B 2011 Plasmonic enhancement of OPTICAL properties by isolated and coupled metal nanoparticles *Plasmonics and Plasmonic Metamaterials* **4** 1–44
[36] Power A C, Byrne S, Goethals S, Betts A J and Cassidy J F 2014 The bench synthesis of silver nanostructures of variable size and an introductory analysis of their optical properties *Aust J Ed Chem.* **73** 1–6
[37] Walshe J, Amarandei G, Ahmed H, McCormack S and Doran J 2019 Development of poly-vinyl alcohol stabilized silver nanofluids for solar thermal applications *Sol. Energy Mater. Sol. Cells* **201** 110085
[38] Han X, Chen X, Wang Q, Alelyani S M and Qu J 2019 Investigation of $CoSO_4$-based Ag nanofluids as spectral beam splitters for hybrid PV/T applications *Sol. Energy* **177** 387–94
[39] Han X, Wang Q and Zheng J 2016 Determination and evaluation of the optical properties of dielectric liquids for concentrating photovoltaic immersion cooling applications *Sol. Energy* **133** 476–84
[40] ASTMG159 1998 Standard tables for references solar spectral irradiance at Air mass 1.5: direct, normal, and hemispherical for a 37° *Tilted Surface ASTM International*
[41] Sultana T, Morrison G, Taylor R and Rosengarten G (ed) Performance of a linear fresnel rooftop mounted concentrating solar collector *Proc. of the 50th Australian Solar Energy Society Annual Conf. (AuSE), Melbourne, Australia; 2012*
[42] The Statistical Office of the European Union (Eurostat) 2018
[43] The Statistical Office of the European Union (Eurostat) 2018 *Natural Gas Price Statistics*
[44] Ilyas S U, Pendyala R and Marneni N 2017 Stability of nanofluids *Engineering applications of nanotechnology* (Berlin: Springer) 1–31
[45] X-f P, X-l Y, L-f X and Zhong 2007 X. Influence factors on suspension stability of nanofluids *Journal-Zhejiang University Engineering Science.* **41** 577
[46] Badi'ah H I, Seedeh F, Supriyanto G and Zaidan A H 2019 *Synthesis of Silver Nanoparticles and the Development in Analysis Method. IOP Conf. Series: Earth and Environmental Science. 2019;217* (https://doi.org/10.1088/1755-1315/217/1/012005)
[47] Jana J, Ganguly M and Pal T 2017 Evolution, stabilization, and tuning of metal-enhanced fluorescence in aqueous solution *Surface Plasmon Enhanced, Coupled and Controlled Fluorescence* (Online Library: Wiley) 9 151–78
[48] Hjerrild N E, Mesgari S, Crisostomo F, Scott J A, Amal R and Taylor R A 2016 Hybrid PV/T enhancement using selectively absorbing Ag–SiO2/carbon nanofluids *Sol. Energy Mater. Sol. Cells* **147** 281–7
[49] Bhattad A and Sarkar J 2021 Effects of nanoparticle shape and size on the thermohydraulic performance of plate evaporator using hybrid nanofluids *J. Therm. Anal. Calorim.* **143** 767–79
[50] CEIC Data 2018 China Electricity Price: 36 City Monthly Average. Accessed date [25/07/21]https://ceicdata.com/en/china/electricity-price-36-city
[51] CEIC Data 2018 China Gas Pricehttps://ceicdata.com/en/china/gas-price